Extracting periodic driving signal from chaotic noise*

MU Jing**, TAO Chao and DU Gonghuan

(State Key Laboratory of Modern Acoustics and Institute of Acoustics, Nanjing University, Nanjing 210093, China)

Received March 10, 2003

Abstract After periodic signals pass through some nonlinear systems, they are usually transformed into noise-like and wide-band chaotic signals. The discrete spectrums of the original periodic signals are often covered by the chaotic spectrums. Recovering the periodic driving signals from the chaotic signals is important not only in theory but also in practical applications. Based on the modeling theory of nonlinear dynamic system, a "polynomial-simple harmonic drive" non-autonomous equation (P-S equation) to approximate the original system is proposed and the approximation error between P-S equation and the original system is obtained. By changing the drive frequency, we obtain the curve of the approximation error vs. drive frequency. Based on the relation between this curve and the spectrums of the original periodic signals, the spectrum of the original driving signal is extracted and the original signal is recovered.

Keywords: non-autonomous system, chaos, chaotic noise.

Chaos has been proved to be an important nonlinear phenomenon universally existing in natural and artificial systems, such as the circumfluence of atmospheric systems[1], nonlinear oscillation systems[2], nonlinear electrocircuits[3], focusing optical fibers[4], the propagation of acoustic ray[5,6] and many other physical systems. At present, chaos has been widely used in various fields[7~10], e.g. chaotic synchronization and chaotic secure communication[8~10] etc. However, the uncontrolled chaos may also do harm to the working of some systems, for example, in complex artificial and natural systems, some uncontrollable nonlinear factors might induce the behavior of the original system into chaos, which will disturb the signal one needs. Therefore the study of chaos control has been developed[11].

The diagram shown in Fig. 1 describes one kind of chaotic system which disturbs the periodic input signal. Periodic signals are turned into noise-like chaotic signals after they pass through some nonlinear transmitting channels, i.e. these nonlinear systems can cover the original periodic input and produce chaotic noise. As a result, extracting and reconstructing

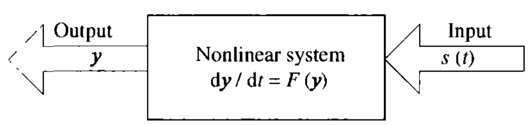

Fig. 1. Nonlinear system.

periodic driving signal from chaotic noise becomes a new subject.

The above phenomenon can be described by the following differential equation:

$$\dot{\boldsymbol{y}} = \boldsymbol{F}(\boldsymbol{y}) + s(t), \tag{1}$$

where $\boldsymbol{y}$ is the state vector of the system and $s(t)$ the periodic driving signal. The system can produce chaos with certain parameters. After periodic signal $s(t)$ passes through the chaotic system, its discrete spectrum can be transformed into wide-band spectrum and the original period is covered by the chaotic noise (Fig.2). It should be noticed that here the chaotic noise is not simply added to the periodic signal, but contrarily, it is generated from the periodic signal by the nonlinear system. Thereby, normal linear methods of extracting periodic signals appear to be ineffective in this kind of situation.

From the above discussion it can be seen that extracting periodic driving signal from chaotic noise is significant for nonlinear dynamical noise reduction, weak signal extraction and deep insight of the chaotic system etc. On the basis of the nonlinear dynamical modeling theory[12~15], this paper investigates a new method of extracting periodic signal from the chaotic output of the non-autonomous chaotic system. In our scheme, we apply a "polynomial-simple harmonic drive" equation (P-S equation) to approximate the original system and use the least square approximation

* Supported by the National Natural Science Foundation of China (Grant Nos. 10074035 and 19834040)

** To whom correspondence should be addressed. E-mail: zhudu@nju.edu.cn

error ε^2 between the P-S equation and the original system as the approximation criteria. The driving frequency of P-S equation is varied within a certain range and the corresponding approximation error is calculated for each of the frequency ω. Then we obtain the curve between the least square approximation error ε^2 and the driving frequency ω. Our theory discovers that there exists a relation between $\varepsilon^2-\omega$ curve and the spectrum of $s(t)$. Based on this theory, the frequency spectrum of the original driving signal can be extracted from the curve $\varepsilon^2-\omega$ and $s(t)$ is recovered from its spectrum without the need of knowing the structure and parameters of the original system.

1 Theory

In practice, one cannot usually observe all the state variables of the system. For example, if only the variable y_1 is observed in Eq. (1), Eq. (1) can be converted into the following standard form by use of some algebraic transformations[12, 13]:

$$\begin{aligned} \dot{y}_1 &= y_2, \\ \dot{y}_2 &= y_3, \\ &\cdots, \\ \dot{y}_{D1} &= g(y_1, y_2, \cdots, y_{D1}) + s(t), \end{aligned} \tag{2}$$

where g is a nonlinear function and $s(t)$ is a driving signal with period T_1. $s(t)$ can be described in the form of Fourier expansion.

$$s(t) = a_0 + \sum_{n=1}^{\infty}(a_n \cos n\omega_1 t + b_n \sin n\omega_1 t),$$

where a_0, a_n and b_n are Fourier coefficients. Thus for an arbitrary periodic driving signal $s(t)$, Eq. (2) can be considered as a non-autonomous system with multi-frequency drive.

We use the following P-S equation to approach the non-autonomous system (2):

$$\begin{aligned} \dot{y}_1 &= y_2, \\ \dot{y}_2 &= y_3, \\ &\cdots, \\ \dot{y}_D &= f(y_1, y_2, \cdots, y_D) + a\cos\omega t + b\sin\omega t, \end{aligned} \tag{3}$$

where y_1 is an observable, and f is a polynomial of an order K:

$$f(y_1, y_2, \cdots, y_D) = \sum_{l_1, l_2, \cdots, l_D=0}^{K} c_{l_1, l_2, \cdots, l_D} \prod_{j=1}^{D} y_j^{l_j},$$

$$\sum_{j=1}^{D} l_j \leqslant K. \tag{4}$$

The polynomial order K and the equation dimension D can be drawn on the results of time series analysis, e.g. the correlation dimension[14]. The discrete time series $v_i = y_1(i\Delta t)$, $i = 1, 2, \cdots, N$ is obtained by sampling the output state variable y_1 of the chaotic system (1), where Δt is the sampling interval. In this paper, our purpose is to recover the periodic driving signal from the observable $\{v_i\}$.

1.1 The method of extracting periodic driving signal

Our method consists of the following three steps:

(i) A series of state vector $\boldsymbol{y}(t_i) = \{(y_1(t_i), y_2(t_i), \cdots, y_n(t_i)\}$ is formed by using the method of successive derivatives[15].

(ii) An initial driving frequency ω_0 of Eq. (3) is selected. Then the least-square technique is used to determine the other coefficients of Eq. (3) and make the Eq. (3) approach Eq. (2), i. e. choosing coefficients $c_{l_1, l_2, \cdots, l_D}$, a and b to minimize the approximation error

$$\begin{aligned} \varepsilon^2(\omega_0) &= \frac{1}{N}\sum_{i=1}^{N}[\dot{y}_D(t_i) \\ &\quad - f(y_1(t_i), y_2(t_i), \cdots, y_D(t_i)) \\ &\quad - a\cos\omega_0 t_i - b\sin\omega_0 t_i]^2, \\ \varepsilon^2(\omega_0) &= \min. \end{aligned} \tag{5}$$

(iii) Varying the driving frequency of Eq. (3) $\omega = \omega_0 + j\Delta\omega$, $j = 1, 2, \cdots, M$ and repeating step (ii), we obtain the approximation error-frequency $(\varepsilon^2_{\min}(\omega) \sim \omega)$ curve. Moreover, we found that the magnitudes of the minimums are related to the Fourier coefficients of the driving signal's spectrum. So the driving signal can be recovered from this curve.

1.2 Relation between $\varepsilon^2_{\min}(\omega) \sim \omega$ curve and power spectrum

ε^2 can be written as follows according to Eq. (5):

$$\varepsilon^2(\omega) = M_1 + 2M_2 + M_3, \tag{6}$$

where

$$\begin{aligned} M_1 &= \frac{1}{N}\sum_{i=1}^{N}[g(y_1(t_i), y_2(t_i), \cdots, y_{D1}(t_i)) \\ &\quad - f(y_1(t_i), y_2(t_i), \cdots, y_D(t_i))]^2, \\ M_2 &= \frac{1}{N}\sum_{i=1}^{N}[g(y_1(t_i), y_2(t_i), \cdots, y_{D1}(t_i)) \\ &\quad - f(y_1(t_i), y_2(t_i), \cdots, y_D(t_i))] \end{aligned}$$

$$\times\Big[a_0+\sum_{n=1}^{\infty}(a_n\cos n\omega_1 t_i+b_n\sin n\omega_1 t_i)$$
$$-(a\cos\omega t_i+b\sin\omega t_i)\Big],$$
$$M_3=\frac{1}{N}\sum_{i=1}^{N}\Big[a_0+\sum_{n=1}^{\infty}(a_n\cos n\omega_1 t_i+b_n\sin n\omega_1 t_i)$$
$$-(a\cos\omega t_i+b\sin\omega t_i)\Big]^2.$$

We have $M_2\approx 0$ as a statistical average value. And according to the mean value theorem, when ε^2 takes a minimum, g approximates f by use of the least square technique, i.e. $M_1\approx 0$. Eq. (6) can be simplified as:

$$\varepsilon^2_{\min}(\omega)=M_3.$$

For an arbitrary integer n, the above equation can be written as:

$$\varepsilon^2_{\min}(\omega)=\frac{1}{N}\sum_{i=1}^{N}\Big[\sum_{j=0,j\neq n}^{\infty}(a_j\cos j\omega_1 t_i+b_j\sin j\omega_1 t_i)\Big]^2$$
$$+\frac{1}{N}\sum_{i=1}^{N}(a_n\cos n\omega_1 t_i+b_n\sin n\omega_1 t_i$$
$$-a\cos\omega t_i-b\sin\omega t_i)^2.$$

This equation is equivalent to the following integral:

$$\varepsilon^2_{\min}(\omega)=\frac{1}{T}\int_0^T\Big[\sum_{j=0,j\neq n}^{\infty}(a_j\cos j\omega_1 t+b_j\sin j\omega_1 t)\Big]^2 dt$$
$$+\frac{1}{T}\int_0^T(a_n\cos n\omega_1 t+b_n\sin n\omega_1 t$$
$$-a\cos\omega t-b\cos\omega t)^2 dt, \qquad (7)$$

where $T=N\Delta t$ is the range of integration. The function on the right-hand side of Eq. (7) can be simplified as:

$$\varepsilon^2_{\min}(\omega)=\begin{cases}\frac{1}{2}\sum_{j=1,j\neq n}^{\infty}(a_j^2+b_j^2)+\frac{1}{2}(a_n^2+b_n^2+a^2+b^2), & \omega\neq n\omega_1,\\ \frac{1}{2}\sum_{j=1,j\neq n}^{\infty}(a_j^2+b_j^2)+\frac{1}{2}(a_n-a)^2+\frac{1}{2}(b_n-b)^2, & \omega=n\omega_1.\end{cases} \qquad (8)$$

According to the least square technique, coefficients a and b satisfy:

$$(a_n-a)^2+(b_n-b)^2\approx 0,\quad \omega=n\omega_1,$$
$$a\approx 0,\ b\approx 0,\quad \omega\neq n\omega_1.$$

So when $\omega=n\omega_1$, the approximation error has a minimum:

$$\varepsilon^2_{\min}(\omega)=\begin{cases}\frac{1}{2}\sum_{j=1}^{\infty}(a_j^2+b_j^2)=\frac{1}{2}\sum_{j=1}^{\infty}A_j^2, & \omega\neq n\omega_1,\\ \frac{1}{2}\sum_{j=1,j\neq n}^{\infty}(a_j^2+b_j^2)=\frac{1}{2}\sum_{j=1,j\neq n}^{\infty}A_j^2, & \omega=n\omega_1,\end{cases} \qquad (9)$$

where $A_j=\sqrt{a_j^2+b_j^2}$ and $\varphi_j=\arctan(b_j/a_j)$ is the corresponding phase angle. This is the relation between the approximation error and ω. The driving signal can be recovered by Eq. (9) and the other parameters of the original system can be recovered by substituting the driving term in the P-S equation with the recovered driving signal if it is necessary.

2 The numerical experiment of extracting the driving signal

2.1 Extracting driving signal with finite frequencies

We illustrate the advantages of our approach using Duffing equation as an example. Duffing equation is a non-autonomous system widely used in the study of nonlinear dynamics. It describes the nonlinear characteristics of dynamic systems and is often met in damping and isolating vibration systems. It can tranfer the driving signal of discrete spectrum into wideband chaotic noise. Generally, an equation with three driving frequencies can be written as:

$$\dot{y}_1=y_2,$$
$$\dot{y}_2=-\gamma_0 y_2-y_1-y_1^3+\sum_{i=1}^{3}A_{i0}\cos\omega_i t. \qquad (10)$$

The parameters in Eq. (10) are $\gamma_0=0.1$, $(A_{i0},\omega_i)=\{(35,1),(40,4),(10,13)\}$. Using the fourth-order Runge-Kutta method with step-size $\Delta t=0.01$, the state variable y_1 of this system is shown in Fig. 2(a). The corresponding spectrum is shown in Fig. 2(b). It can be seen that the original periodic signals are covered by the chaotic noise.

The least square approximation error can be obtained by using Eq. (3) to approximate the time series y_1, as is shown in Fig. 3. Since A_{30} is smaller than A_{10} by 25 dB and smaller than A_{20} by 27.7 dB, the third minmum in Fig. 3 is a little shallow comparatively. The enlarged figure of the third minimum is also given in Fig. 3.

In the above theoretical analysis (see Eq. (9)) when $\omega=n\omega_1$, there is a jump to a minimum but in

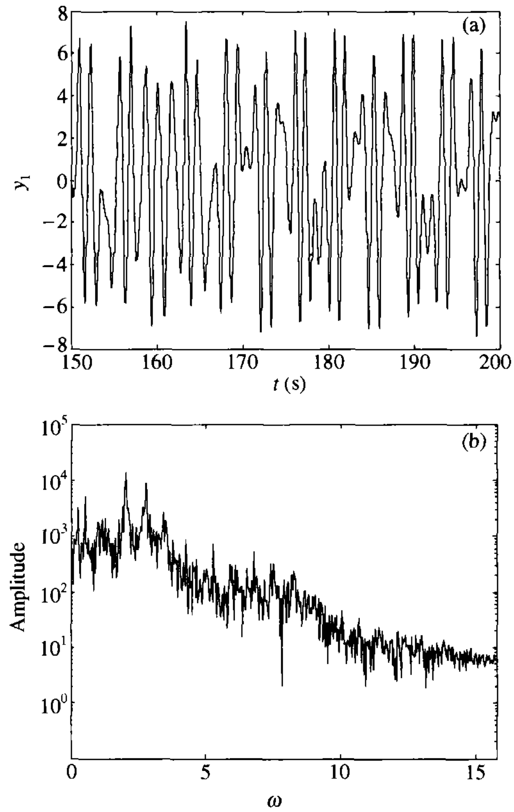

Fig. 2. The response in the time domain (a); and the corresponding spectrum of the response (b).

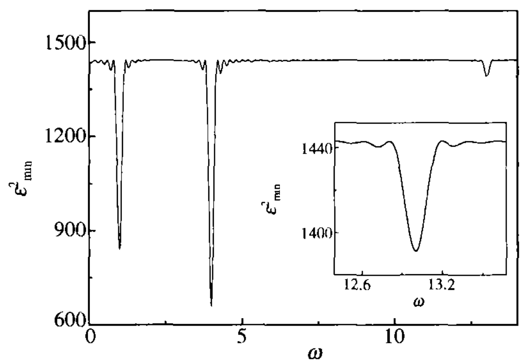

Fig. 3. $\varepsilon^2_{\min}(\omega) \sim \omega$ curve.

the remained area the approximation error is constant. The three minimums which correspond to the three driving frequencies can be seen very clearly in Fig. 3. However, there are some small fluctuations near the three minimums, which is caused by the truncation and round-off error in numerical computation. These fluctuations can be ignored for their amplitudes are much smaller than the nearby minimums.

According to Eq. (9), we have the following results derived from Fig. 3.

$$\omega_1 = 1.0007, \quad \omega_2 = 4.0023, \quad \omega_3 = 12.9932,$$

$$\langle \varepsilon^2_{\min}(\omega_1) \rangle = \frac{1}{2}(A_2^2 + A_3^2) = 843.6712, \quad (11)$$

$$\langle \varepsilon^2_{\min}(\omega_2) \rangle = \frac{1}{2}(A_1^2 + A_3^2) = 679.0616, \quad (12)$$

$$\langle \varepsilon^2_{\min}(\omega_3) \rangle = \frac{1}{2}(A_2^2 + A_1^2) = 1418.9572. \quad (13)$$

The solutions of Eqs. (11) ~ (13) are:

$$A_1 = 35.4168, \quad A_2 = 39.7941, \quad A_3 = 10.1870.$$

From the above example, it can be seen that the frequency and the corresponding amplitude of the driving signal can be recovered more accurately. If necessary, we can also estimate the parameter of system $\gamma_0 = 0.1011$ by Eq. (3). To check the similarity between the original system and the P-S equation, the phase space of the original system is demonstrated in Fig. 4(a), which is derived from the observed state variable y_1 and y_2 ($y_2 = \dot{y}_1$). Fig. 4(b) is the recovered phase space derived from the above method. It can be seen that the states of the two systems are very similar.

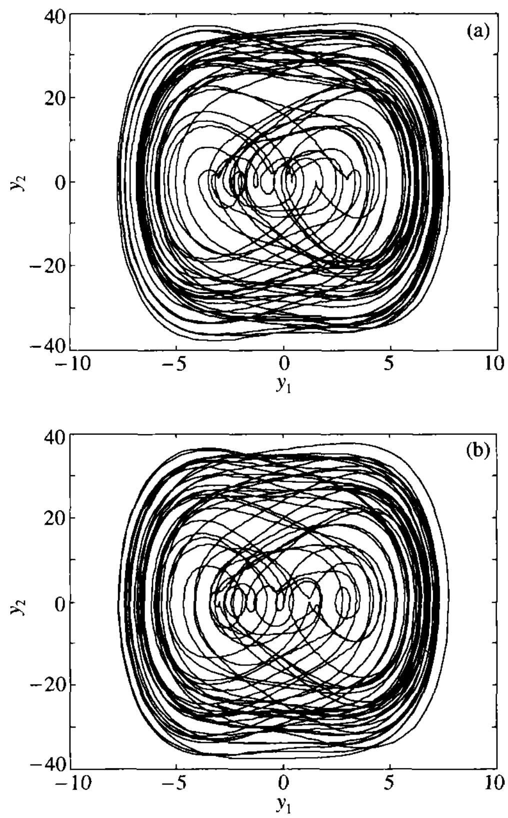

Fig. 4. The phase space of the original system (a) and the phase space recovered by Eq. (3) (b).

2.2 Extracting the periodic pulse train

Further, a periodic pulse train is used as the driving signal, which actually is a driving signal composed of infinite frequencies. A Duffing equation driven by the periodic rectangular-shaped pulse train can be written as:

$$\dot{y}_1 = y_2,$$
$$\dot{y}_2 = -\gamma_0 y_2 - y_1 - y_1^3 + d(t), \qquad (14)$$

where parameter $\gamma_0 = 0.1$ and

$$d(t) = \begin{cases} E & (|t/(2\pi) - n| \leqslant 0.05,\ n = 0, 1, 2, \cdots) \\ 0 & (|t/(2\pi) - n| > 0.05,\ n = 0, 1, 2, \cdots) \end{cases}.$$

The period of the rectangular-shaped pulse train is $T = 2\pi$. The pulse width is $\tau = \pi/5$ and its height is $E = 178$. The Fourier expansion of $d(t)$ can be written in the form of

$$d(t) = \frac{E\tau}{T} + \frac{2E\tau}{T}\sum_{n=1}^{\infty} Sa\left(\frac{n\pi\tau}{T}\right)\cos\left(n\frac{2\pi}{T}t\right),$$

where Sa is the sampling function. The former six terms on the right-hand side of the above equation of $d(t)$ can be expanded as follows.

$$d(t) = A_{10} + A_{20}\cos t + A_{30}\cos 3t + A_{40}\cos 5t - A_{50}\cos 7t + A_{60}\cos 9t + \cdots,$$

where the "true" amplitudes are:

$A_{10} = 17.7912$, $A_{20} = 35.0000$, $A_{30} = 33.2870$, $A_{40} = 30.5437$, $A_{50} = 26.9297$, $A_{60} = 22.6525, \cdots$.

We integrate Eq. (14) and obtain the time series y_1. Then we use Eq. (3) to approximate the time series y_1 of Eq. (14) and scan ω within $[0, 82]$. Thus the relation curve between the least square approximation error $\varepsilon^2_{\min}(\omega)$ and ω is obtained, as shown in Fig. 5.

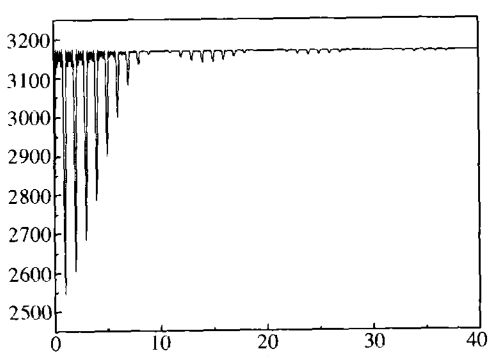

Fig. 5. The relationship between the least square approximation error $\varepsilon^2_{\min}(\omega)$ and ω.

It can be seen clearly that the distribution of the minimal values in Fig. 5 is very similar to the spectrum of the rectangular-shaped pulse train. According to the analysis in the second section, using the minimal values in Fig. 5 we can determine their corresponding frequencies and amplitudes. This is compared with the spectrum of the original driving signal in Fig. 6(a). The bars in Fig. 6 are the spectrum of the original driving signal and the dotted line is the recovered spectrum of the driving signal respectively. They are quite close to each other. We can also obtain the phase angle of the driving signal, which is shown in Fig. 6(b).

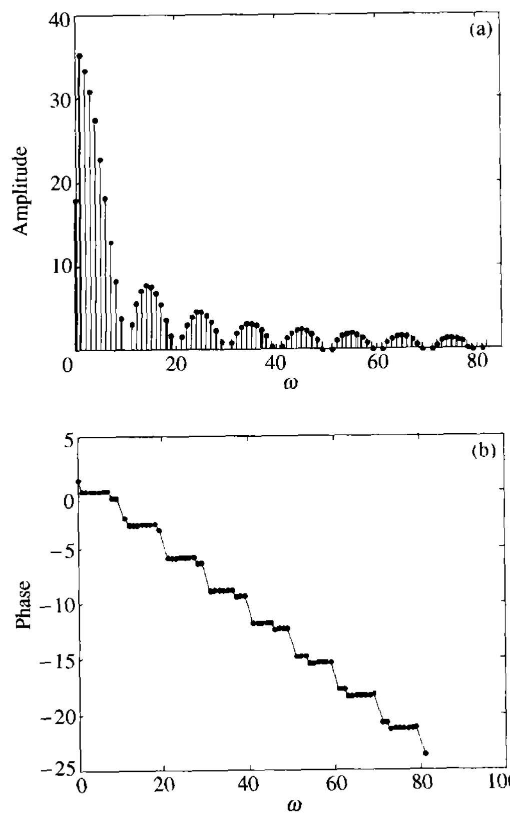

Fig. 6. The spectrum of the original driving signal and the recovered spectrum (a). The bars are the spectrum of the original driving signal and the dots are the recovered spectrum. (b) The recovered phase angle of the driving signal.

The driving signal is recovered from the amplitude and phase angle given in Fig. 6. It is shown in Fig. 7(b). Fig. 7(a) gives the waveform of the original driving signal. It can be concluded from Fig. 7 that the driving signal can be recovered efficiently.

From the above analysis, it can be concluded that an arbitrary periodic driving signal can be effectively recovered by our approach.

3 Conclusion

We explored theoretically the approach of using the P-S equation to extract driving signals from

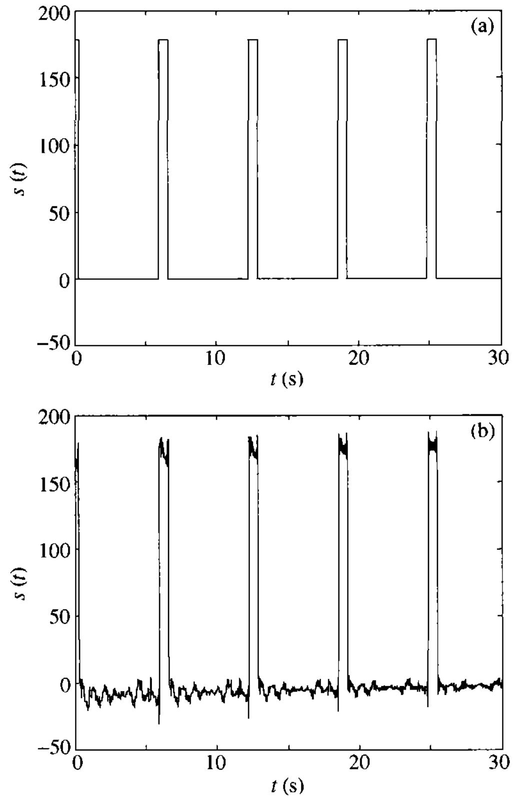

Fig. 7. The original driving signal (a) and the recovered driving signal (b).

chaotic noise. The relationship between the approximation error and the frequency is obtained by scanning the frequency. The spectrum of the driving signal is computed according to the relation between the approximation error curve and the power spectrum of the driving signal. The remained parameters of the system can also be determined if necessary. Numerical experiment result shows that this approach can extract the periodic driving signal from the chaotic noise generated by non-autonomous chaotic systems effectively. This verifies our theory successfully.

References

1 Lorenz, E. N. Deterministic non-periodic flow. J. Atmospheric. Sci., 1963, 20: 130.

2 Jiang, J. J. et al. Modeling of chaotic vibrations in symmetric vocalfolds. J. Acoust. Soc. Am., 2001, 110(4): 2120.

3 Sprott, J. C. A new class of chaotic circuit. Phys. Rev. A, 2000, 266: 19.

4 Li, X. et al. Study on chaotic behavior of optical ray in a focusing fiber. J. Opt. Soc. Am., 2001, 18: 318.

5 Li, X. et al. Influence of perturbations on chaotic behavior of the parabolic ray system. J. Acoust. Soc. Am., 1999, 4: 105.

6 Frison, T. W. et al. Nonlinear analysis of environmental distortions of continuous wave signals in the ocean. J. Acoust. Soc. Am., 1996, 99(1): 139.

7 Liang, J. et al. Extraction and application of low dimensional dynamical component from underwater acoustic target radiated noise. Chinese Journal of Acoustics, 2001, 20(4): 319.

8 Pecora, L. M. et al. Synchronization in chaotic systems. Phys. Rev. Lett., 1990, 64: 821.

9 Xiao, J. H. et al. Synchronization of spatiotemporal chaos and its application to multichannel spread-spectrum communication. Phys. Rev. Lett., 1996, 77: 4162.

10 Murali, K. Digital signal transmission with cascaded heterogeneous chaotic system. Phys. Rev. E, 2000, 63: 016217.

11 Ott, E. et al. Controlling chaos. Phys. Rev. Lett., 1990, 64: 1196.

12 Bezruchko, B. P. et al. Constructing nonautonomous differential equations from experimental time series. Phys. Rev. E, 2000, 63: 016207-1-7.

13 Gouesbet, G. et al. Global vector-field reconstruction by using a multivariate polynomial L_2 approximation on nets. Phys. Rev. E, 1993, 49(6): 4955.

14 Bezruchko, B. P. et al. Role of transient process for reconstruction of model equations from time series. Phys. Rev. E, 2001, 64: 036210.

15 Gouesbet, G. et al. Construction of phenomenological models from numerical scalar time series. Physica D, 1992, 58: 202.